AFRL-RX-TY-TP-2011-0081

ENZYMATIC FUEL CELLS: INTEGRATING FLOW-THROUGH ANODE AND AIR-BREATHING CATHODE INTO A MEMBRANE-LESS BIOFUEL CELL DESIGN

Rosalba A. Rincón, Carolin Lau, Kristen E. Garcia, Emily Adkins,
Plamen Atanassov
Department of Chemical & Nuclear Engineering
University of new Mexico
Albuquerque, NM 87131

Heather R. Luckarift
Universal Technology Corporation
1270 North Fairfield Drive
Dayton, OH 45432

Glenn R. Johnson
Airbase Technologies Division
Air Force Research Laboratory
139 Barnes Drive, Suite 2
Tyndall Air Force Base, FL 32403-5323

Contract No. FA8650-07-D-5800-0037

June 2011

AIR FORCE RESEARCH LABORATORY
MATERIALS AND MANUFACTURING DIRECTORATE

■ **Air Force Materiel Command** ■ **United States Air Force** ■ **Tyndall Air Force Base, FL 32403-5323**

REPORT DOCUMENTATION PAGE

Form Approved
OMB No. 0704-0188

PLEASE DO NOT RETURN YOUR FORM TO THE ABOVE ADDRESS.

1. REPORT DATE *(DD-MM-YYYY)*	2. REPORT TYPE	3. DATES COVERED *(From - To)*
01-JUN-2011	Journal Article (POSTPRINT)	01-JAN-2010 -- 31-JAN-2011

4. TITLE AND SUBTITLE

Enzymatic Fuel Cells: Integrating Flow-Through Anode and Air-Breathing Cathode Into a Membrane-Less Biofuel Cell Design (POSTPRINT)

5a. CONTRACT NUMBER

FA8650-07-D-5800-0037

5b. GRANT NUMBER

5c. PROGRAM ELEMENT NUMBER

0602102F

6. AUTHOR(S)

*Rincón, Rosalba A.; *Lau, Carolin; **Luckarift, Heather R.; *Garcia, Kristen E.; *Adkins, Emily; #Johnson, Glenn R.; *Atanassov, Plamen

5d. PROJECT NUMBER

GOVT

5e. TASK NUMBER

L0

5f. WORK UNIT NUMBER

Q140LA62

7. PERFORMING ORGANIZATION NAME(S) AND ADDRESS(ES)

*Department of Chemical & Nuclear Engineering, University of New Mexico, Albuquerque, NM 87131;
** Universal Technology Corporation, 1270 North Fairfield Drive, Dayton, OH 45432

8. PERFORMING ORGANIZATION REPORT NUMBER

9. SPONSORING/MONITORING AGENCY NAME(S) AND ADDRESS(ES)

Air Force Research Laboratory
Materials and Manufacturing Directorate
Airbase Technologies Division
139 Barnes Drive, Suite 2
Tyndall Air Force Base, FL 32403-5323

10. SPONSOR/MONITOR'S ACRONYM(S)

AFRL/RXQL

11. SPONSOR/MONITOR'S REPORT NUMBER(S)

AFRL-RX-TY-TP-2011-0081

12. DISTRIBUTION/AVAILABILITY STATEMENT

Distribution Statement A. Approved for public release; distribution unlimited.

13. SUPPLEMENTARY NOTES

Ref Public Affairs Case # 88ABW-2011-2228, 14 Apr 11. Document contains color images.

14. ABSTRACT

One of the key goals of enzymatic biofuel cells research has been the development of a fully enzymatic biofuel cell that operates under a continuous flow-through regime. Here, we present our work on achieving this task. Two NAD+-dependent dehydrogenase enzymes; malate dehydrogenase (MDH) and alcohol dehydrogenase (ADH) were independently coupled with poly-methylene green (poly-MG) catalyst for biofuel cell anode fabrication. A fungal laccase that catalyzes oxygen reduction via direct electron transfer (DET) was used as an air-breathing cathode. This completes a fully enzymatic biofuel cell that operates in a flow-through mode of fuel supply polarized against an air-breathing bio-cathode. The combined, enzymatic, MDH-laccase biofuel cell operated with an open circuit voltage (OCV) of 0.584 V, whereas the ADH-laccase biofuel cell sustained an OCV of 0.618 V. Maximum volumetric power densities approaching 20 mW cm-3 are reported, and characterization criteria that will aid in future optimization are discussed.

15. SUBJECT TERMS

Biofuel cell, Flow-through, Air-breathing cathode, NAD+-dependent enzyme, Poly-methylene green, Membrane-less

16. SECURITY CLASSIFICATION OF:			17. LIMITATION OF ABSTRACT	18. NUMBER OF PAGES	19a. NAME OF RESPONSIBLE PERSON
a. REPORT	b. ABSTRACT	c. THIS PAGE			Glenn R. Johnson
U	U	U	UU	6	19b. TELEPHONE NUMBER *(Include area code)*

Reset

Standard Form 298 (Rev. 8/98)
Prescribed by ANSI Std. Z39.18

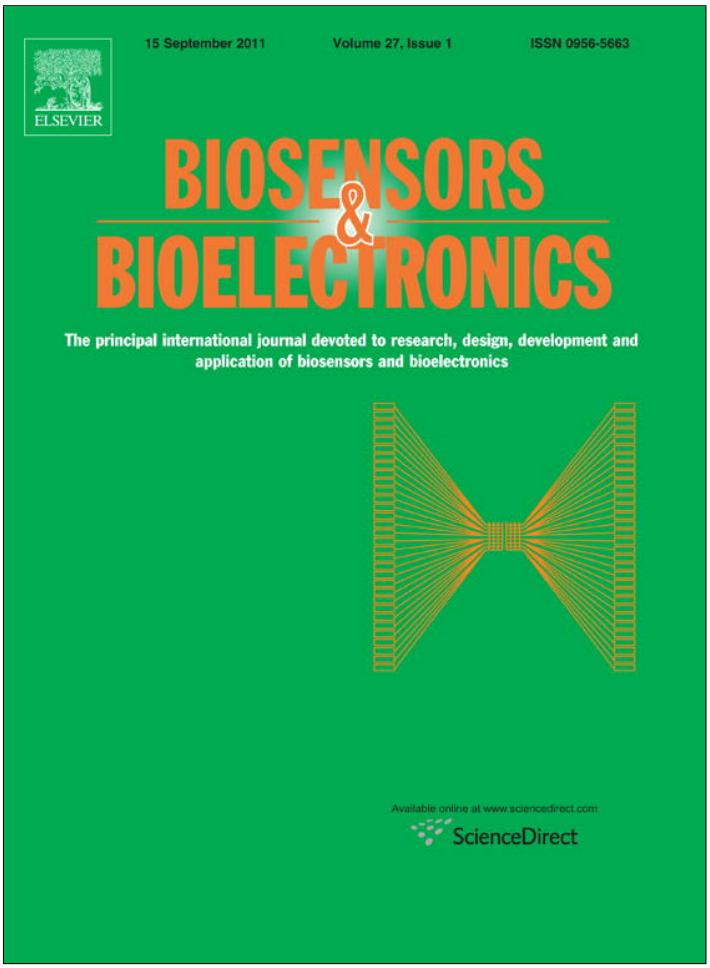

Biosensors and Bioelectronics 27 (2011) 132–136

Contents lists available at ScienceDirect

Biosensors and Bioelectronics

journal homepage: www.elsevier.com/locate/bios

Enzymatic fuel cells: Integrating flow-through anode and air-breathing cathode into a membrane-less biofuel cell design

Rosalba A. Rincón[a], Carolin Lau[a], Heather R. Luckarift[b,c], Kristen E. Garcia[a], Emily Adkins[a], Glenn R. Johnson[b], Plamen Atanassov[a,*]

[a] Department of Chemical & Nuclear Engineering, Center for Emerging Energy Technologies, University of New Mexico, Albuquerque, NM 87131, USA
[b] Microbiology and Applied Biochemistry (AFRL/RXQL), Air Force Research Laboratory, 139 Barnes Drive, Suite #2, Tyndall Air Force Base, FL 32403, USA
[c] Universal Technology Corporation, 1270 North Fairfield Drive, Dayton, OH 45432, USA

ARTICLE INFO

Article history:
Received 28 February 2011
Received in revised form 24 May 2011
Accepted 26 June 2011
Available online 2 July 2011

Keywords:
Biofuel cell
Flow-through
Air-breathing cathode
NAD^+-dependent enzyme
Poly-methylene green
Membrane-less

ABSTRACT

One of the key goals of enzymatic biofuel cells research has been the development of a fully enzymatic biofuel cell that operates under a continuous flow-through regime. Here, we present our work on achieving this task. Two NAD^+-dependent dehydrogenase enzymes; malate dehydrogenase (MDH) and alcohol dehydrogenase (ADH) were independently coupled with poly-methylene green (poly-MG) catalyst for biofuel cell anode fabrication. A fungal laccase that catalyzes oxygen reduction via direct electron transfer (DET) was used as an air-breathing cathode. This completes a fully enzymatic biofuel cell that operates in a flow-through mode of fuel supply polarized against an air-breathing bio-cathode. The combined, enzymatic, MDH-laccase biofuel cell operated with an open circuit voltage (OCV) of 0.584 V, whereas the ADH-laccase biofuel cell sustained an OCV of 0.618 V. Maximum volumetric power densities approaching 20 $\mu W\,cm^{-3}$ are reported, and characterization criteria that will aid in future optimization are discussed.

1. Introduction

Interest in energy harvesting devices based on alternative fuels has exponentially increased over the last two decades. Researchers have increasingly drawn their attention to biological fuel cells in recent years, seeing that conventional fuel cell technologies are reaching mass-market introduction. Reasons for this shift in interest are based on unique conditions of operation that cannot be met by conventional fuel cells; namely low-temperature operation (20–40 °C) activity near neutral pH, and selective catalytic activity. Moreover, biofuel cells can utilize a wide diversity of fuel sources and a multitude of biocatalysts. They also offer low costs for operation and maintenance in comparison with conventional fuel cells (Barton et al., 2004; Davis and Higson, 2007; Heller, 2004; Minteer et al., 2007). Specifically, enzymatic biofuel cells have the capability of producing power densities higher than those observed for microbial fuel cells. In definition, an enzymatic biofuel cell uses enzymes as catalysts for both its anodic and cathodic reactions.

The thermodynamic driving force of biofuel cells is directly related to the electron transfer mechanism of the processes occurring at the anode and cathode. In general, these can be classified into two mechanisms: mediated electron transfer (MET), and direct electron transfer (DET) (Barton et al., 2001a,b, 2002, 2004; Chen et al., 2001; Katz et al., 2003). In MET, a low molecular weight redox-active molecule (mediator) is included in electrolyte to shuttle electrons between the active site of the enzyme and the electrode surface. The use of redox mediators, however, can decrease the potential of the electrode and therefore limit the driving force between the anode and the cathode. Mediators also have some stability and toxicity issues, which is why in recent years research has focused on achieving direct electrical communication between redox centers and electrodes (Barton et al., 2004; Ghindilis et al., 1997; Shleev et al., 2005). By achieving DET, the electrode can work at a potential range close to the redox potential of the enzyme itself (Shleev et al., 2005).

In previous studies, we have successfully demonstrated the development of enzymatic gas-diffusion cathodes based on DET of oxygen reduction catalysts, such as laccase (Gupta et al., 2011a,b). The methodology of cathode fabrication provides efficient enzyme-electrode communication, minimizes ohmic resistance losses, and maximizes oxygen supply under "air-breathing" conditions (Shleev et al., 2005).

Enzymatic bioelectro-reduction of oxygen at the cathode, in this manner, is reported for copper-containing oxidases such as laccase, ascorbate oxidase, and bilirubin oxidase (Gupta et al., 2011a,b;

* Corresponding author. Tel.: +1 505 277 2640; fax: +1 505 277 5433.
E-mail address: plamen@unm.edu (P. Atanassov).

0956-5663/$ – see front matter © 2011 Elsevier B.V. All rights reserved.
doi:10.1016/j.bios.2011.06.029

Ivnitski et al., 2008, 2010; Ivnitski and Atanassov, 2007; Solomon et al., 1996). Laccase belongs to the group of multicopper oxidases that catalyze the four-electron reduction of oxygen to water, while oxidizing a wide range of aromatic substrates (Piontek et al., 2002). In addition, laccase enzymes possess high thermodynamic potential and catalytic parameters that are optimal for the development of cathodes for biofuel cells (Barton et al., 2004; Mano et al., 2006; Solomon et al., 1992, 1996). Spectroscopic studies and X-ray crystallography reveal that laccase proteins include a minimal functional unit containing one blue copper, Type 1 (T1) site, and a trinuclear cluster that has one Type 2 and two Type 3 copper atoms (T2/T3) (Piontek et al., 2002; Shleev et al., 2005; Solomon et al., 1992, 1996). The T1 center provides long-range intramolecular rapid electron transfer from the substrate, redox mediator or electrode to the trinuclear T2/T3 redox copper center, where oxygen reduction to water takes place, via intermolecular electron transfer (Piontek et al., 2002; Solomon et al., 1992, 1996; Xu et al., 1996). Fungal laccases in particular, are capable of reducing oxygen at high potentials (680–850 mV) (Barton et al., 2004, 2002; Morozova et al., 2007; Piontek et al., 2002; Reinhammar, 1972; Shleev et al., 2005; Xu et al., 1996) but their activity is often optimal at low pH (4–5) and reduced, or even inactive, at neutrality; the desirable operating pH for biofuel cells (Barton et al., 2004).

For biofuel cell anode design a wide range of enzymes can be explored, since a variety of fuels can be used. Considering the oxidation of glucose as a model fuel, for example, a multitude of enzymes is able to catalyze the first-step of glucose oxidation. These enzymes utilize different cofactors (e.g., nicotinamide adenine dinucleotide, NAD^+; flavin adenine dinucleotide, FAD; or pyrroloquinoline quinone, PQQ), which define the reaction redox potentials. NAD^+-dependent enzymes are known to have the lowest redox potential. Since one would like to work at the lowest anode potential in order to obtain the maximum cell voltage, the use of NAD^+-dependent enzymes is highly desirable. There are several NAD^+-dependent enzymes that are involved in metabolic pathways like the Kreb's cycle and glycolysis. We have selected two model enzymes for this research: malate dehydrogenase (MDH) and alcohol dehydrogenase (ADH).

Historically, the use of NAD^+-dependent enzymes as the anode of biofuel cells has been limited by the need to reoxidize NADH in order to regenerate the enzyme cofactor. Mediators and catalysts have been demonstrated in order to address this issue, but to date have only been used in biofuel cells that operate in a "quiescent" mode, which results in insufficient transport of fuels and thus limited conversion (Palmore et al., 1998). We have recently reported the development of poly-(methylene green) electrocatalysts for NADH oxidation, however, that can be fabricated directly onto 3-dimensional (3D) electrode materials (Rincón et al., 2011). By combining such structures with defined enzyme immobilization techniques we have been able to obtain anodic electrodes that can support continuous flow regimes. The use of 3D chitosan scaffolds, for example, makes it possible to entrap NAD^+-dependent enzymes and retain catalytic activities (Cooney et al., 2008, 2009; Lau et al., 2008, 2010). Moreover, chitosan can be combined with carbon nanotubes (CNTs) to obtain micro-porous polymeric scaffolds that provide a high residence time for the diffusive cofactor (NAD^+), resulting in efficient electrochemical conversion of NADH and in turn, good conversion of the fuel (Martin et al., 2010; Rincón et al., 2011). This immobilization technique has been previously studied and chosen due to its ability to provide enhanced enzymatic activity and stability.

For the research described herein, we utilize a standardized laboratory platform that serves as a stackable, flow-through, fuel cell system (Svoboda et al., 2008) in which both bio-anode and biocathode were integrated with the purpose of generating power from biological fuels.

Completing a fully enzymatic biofuel cell requires the design of an anode that is functional in flow-through mode of the fuel (and potentially the electrolyte) with a cathode capable of operating in a gas-flow mode. It is preferred those flow modes to impose as low parasitic loss as possible. In this research the air-breathing gas-diffusion enzyme-catalyzed electrode of hydrophobic type is being incorporated as a passive cathode. This paper presents the effort and investment of our team in engineering both anode and cathode for an enzymatic biofuel cell that is able to operate in a continuous flow mode. The following sections describe the development of a cathode that can undergo DET and a 3D anode that is based on NAD^+-dependent enzymes.

2. Material and methods

2.1. Materials

Methylene green (Fluka Cat. 66870), L-(−)-malic acid (Sigma Cat. M1000), NADH (Sigma Cat. N6005), NAD^+ (Fluka Cat. 43407), alcohol dehydrogenase (ADH) from *Saccharomycescerevisiae* (pI: 5.4–5.8, Sigma Cat. A3263, 347 U mg^{-1}), laccase from *Trametes versicolor* (pI: 4.1–4.7, Sigma Cat. 53739, 25.5 U mg^{-1}), chitosan (CHIT) (medium molecular weight, Aldrich Cat. 448877), ethanol (200 proof, VWR Cat. 89125172), multi-walled carbon nanotubes (MWCNTs) (20–30 nm outer diameter, 10–30 μm length, 95 wt% purity from www.cheaptubesinc.com), dimethyl sulfoxide (DMSO, Sigma), 1-pyrenebutyric acid N-hydroxysuccinimide ester (PBSE 95%, Sigma–Aldrich Cat. 457078), carbon black (XC72R, Cabot), and concentrated acetic acid (EMD Chemicals Cat. EMAX0073P5) were used without further purification. All other chemicals were reagent grade quality. Malate dehydrogenase (MDH) from porcine heart (pI: 6.1–6.4, USB products from Affymetrix Cat. 18665, 2580 U mg^{-1}) was purified by dialysis (Slide-A-Lyzer MINI dialysis units 10,000 MWCO, and concentrating solution from Thermo Scientific) with TRIS buffer (pH 7.0, 50 mM) in three steps (30 min, 1 h and 30 min) against 500 mL of the same buffer. The final MDH stock solution contained 1 mg MDH/10 μL TRIS buffer (pH 7.0). Chitosan was pretreated to achieve a final deacetylation degree of 95% by initially autoclaving (20 min at 121 °C in 40 wt% NaOH), followed by filtration and washing with DI water and phosphate buffer (pH 8.0, 0.1 M) before drying in a vacuum oven at 50 °C for 24 h. A MWCNTs/CHIT suspensionwas prepared by combining 1 wt% CHIT (in 0.25 M acetic acid) stock solution and MWCNTs (final concentration of 2.5 wt%). NADH stock solutions were prepared for each buffer. L-malic acid was prepared with distilled water and its pH was adjusted to 7.4 with concentrated NaOH.

Electrochemical measurements were carried out using a stackable flow through electrochemical cell (Svoboda et al., 2008) with a platinum mesh (100 mesh, Alfa Aesar Cat. 10282) counter electrode and Ag/AgCl/sat KCl reference electrode (CH Instruments Inc.) when working in the three-electrode setup. For the fuel cell experiments (two-electrode setup) the cathode was connected to the potentiostat as the working electrode and the anode was connected as the counter and reference electrodes. All potential values are reported against Ag/AgCl.

2.2. Preparation of dehydrogenase anodes

Reticulated vitreous carbon (RVC) of a defined porosity (60 pores per linear inch, ppi) was used for the anode supporting material and was pretreated with oxygen plasma cleaning for 15 s to achieve hydrophilization of the surfaces. Enzymatic anodes were prepared by modifying 60 ppi RVC with poly-(MG) as previously described, with10 deposition cycles (Rincón et al., 2011). The immobilization technique for both enzymes (MDH and ADH)

was direct entrapment in the MWCNTs/CHIT scaffolds according to procedures presented by Cooney et al. (2008, 2009) and Lau et al. (2008, 2010). Briefly, materials were prepared by filling the RVC electrodes with CHIT/MWCNTs/NAD^+/MDH (500 μL of immobilization solution in which every10 μL of chitosan contain 0.35 mg NAD^+ and 1 μL MDH or 3 μL ADH) and then frozen at −4 °C overnight. Freeze-drying was performed for 4 h in order to eliminate water from the scaffold. The stock solutions of enzymes contained 1 mg of enzyme per 10 μL of buffer, hence the MDH anode contained 5 mg of enzyme, and the ADH anode contained 15 mg of enzyme. The amount of ADH immobilized to electrodes was calculated based on the amount of enzyme units in order to obtain comparable results to those for MDH.

2.3. Preparation of laccase cathode

The gas-diffusion cathode consists of two layers: a gas diffusion layer and a catalytic layer. 80 mg of carbon black XC72R with a Teflon content of 35 wt% were placed into a round dye (2 cm diameter) and pressed by hand onto a nickel mesh (Alfa Aesar Cat. 39704) that serves as current collector. 10 mg of teflonized multi-walled carbon nanotubes (3.5 wt% PTFE) were evenly distributed on top of the gas diffusion layer. The layers were fused by pressing (1 min at 1 kp) in a hydraulic press to a final thickness of 0.5 mm. PBSE (1-pyrenebutyric acid N-hydroxysuccinimide ester) (4 mg in 0.5 mL DMSO) was allowed to soak into the catalytic layer for 2 h, before the electrode was rinsed with DMSO and then with DI water. Laccase was immobilized by physical adsorption onto the electrode by incubating 0.5 mL of the enzyme (4 mg mL^{-1} in PBS, pH 6.3) at +4 °C overnight. The electrode was rinsed with DI after incubation.

2.4. Enzymatic biofuel cell construction

Fig. 1 shows the fuel cell assembly consisting of the laccase-cathode (lower plate), two counter electrodes (platinum mesh), the dehydrogenase-anode and a reference electrode. The cell was setup in this configuration so that both the anode and cathode could be studied independently and their individual polarization curves determined before measuring the output of the complete, functioning fuel cell. For the ADH-laccase fuel cell, the fuel solution consisted of 475 mM ethanol and 1.5 mM NAD^+, and for the MDH-laccase fuel cell, the fuel solution contained 500 mM L-malate and 1.5 mM NAD^+. Polarization curves were constructed for the cathode (under potentiostatic regime) and for the complete biofuel cell (under potentiostatic and galvanostatic regimes). The anodic polarization curve was determined by subtracting the cathodic curve from the fuel cell curve. The fuel was pumped to the fuel cell using a peristaltic pump at a flow rate of 3 mL/min and the fuel was recycled back into the fuel cell. This flow speed was chosen as optimal after different trials. It provides enough flow of the fuel, without compromising the mechanical stability of the electrodes.

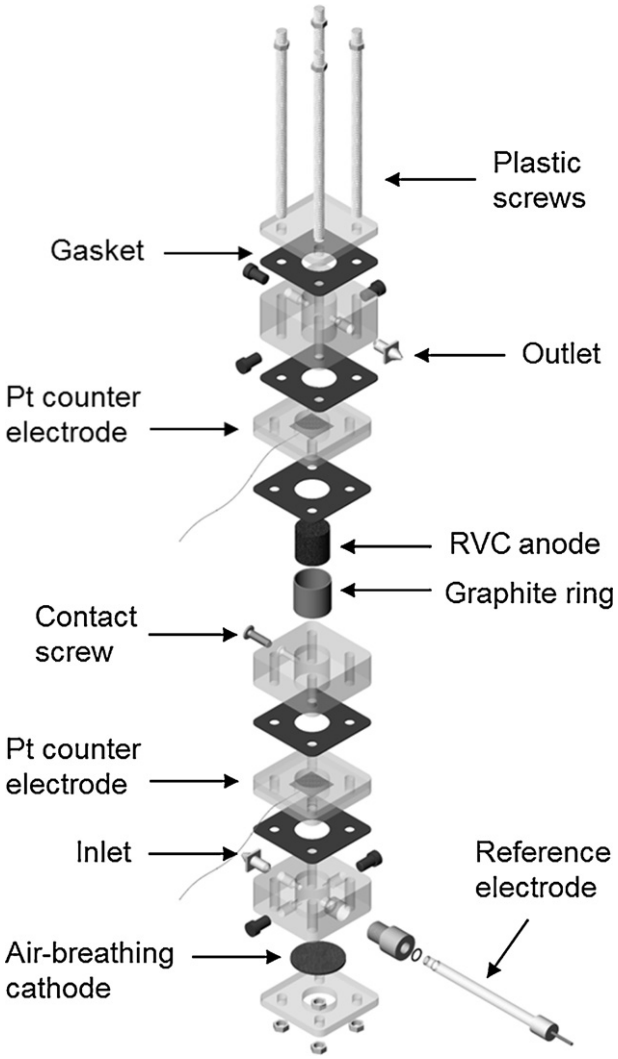

Fig. 1. Schematic of biofuel cell assembly.

3. Results and discussion

3.1. MDH-laccase biofuel cell

The working parameters of a functional fuel cell can be defined from polarization curves, obtained under both galvanostatic and potentiostatic regimes.

Initially, an open circuit voltage (OCV) of 0.584 V was observed for the MDH-laccase biofuel cell (Fig. 2). The shape of the polarization curve for the anode indicates that the MDH-anode is limited by ohmic losses and transport limitations. The laccase-cathode in comparison, demonstrates minimal kinetic losses within the current operation range of the anode. The biofuel cell polarization curve, therefore, shows a kinetic-limited behavior for currents lower than

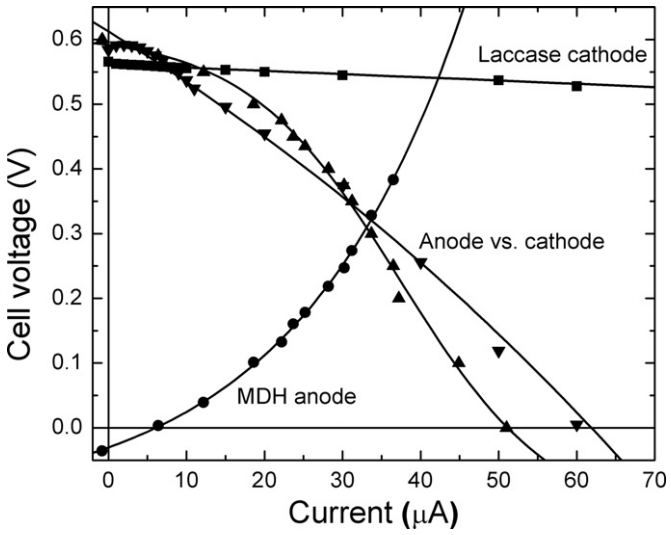

Fig. 2. Polarization curves of: (●) MDH-anode, (■) laccase-cathode, and (▲ potentiostatic, ▼ galvanostatic) biofuel cell. L-malate concentration: 500 mM. OCV = 0.584 V.

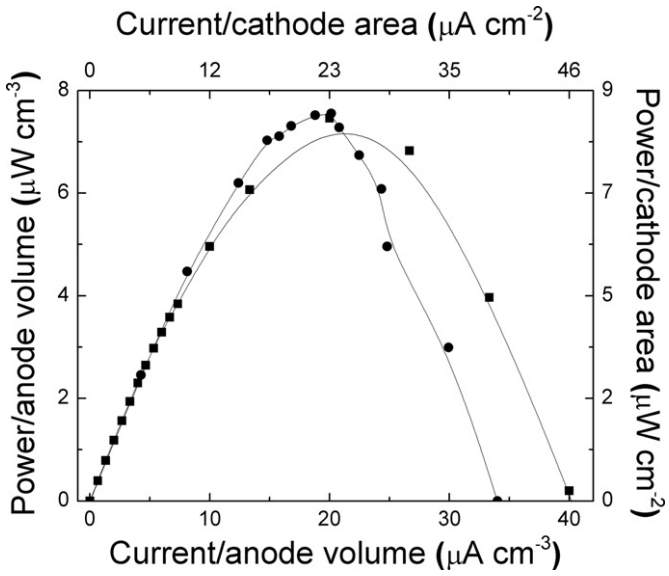

Fig. 3. Power curves of MDH-laccase biofuel cell in 500 mM L-malate normalized to anode volume and cathode area: (■) galvanostatic, (♦) potentiostatic.

10 μA where the sustained voltage is almost independent of the current. At currents higher than 10 μA, ohmic losses are observed and the limitations of the anode dictate the overall performance of the biofuel cell and restrain maximum current to about 65 μA.

Clearly, for the case of biofuel cells, evaluation of the system under galvanostatic regime is more informative, as we are interested in observing the voltage output that the complete fuel cell can sustain. It was necessary, however, to perform the potentiostatic experiments in order to determine the operational range of the device, in respect to current.

Fig. 3 shows power curves that were constructed for the MDH-laccase biofuel cell, represented with the volume of the anode (~1.5 cm^3)and area of the cathode (~1.3 cm^2)taken into account. A maximum power density of ~9 μW cm^{-2} was observed, in good agreement with reports for enzymatic biofuel cells based on a single dehydrogenase enzyme in mediated systems (Stoica et al., 2009).

The maximum power per unit volume (of the anode) was ~8 μW cm^{-3}. Current biofuel cell methodologies often report maximum current and power outputs based on per unit area, but reporting outputs per unit volume is more significant for 3-D architectures and provides a design parameter for scale-up of the biofuel cell technology.

3.2. ADH-laccase biofuel cell

A second biofuel cell was designed with the laccase-cathode as above but with an ADH-anode. Fig. 4 shows the open circuit potentials obtained for each electrode, as well as the cell voltage data. The open circuit potential (OCP) of the anode approached −0.05 V vs. Ag/AgCl while the OCP of the cathode approaches 0.58 V vs. Ag/AgCl. In combination, this provides a theoretical maximum cell voltage of 0.63 V for the biofuel cell. In fact, Fig. 4 shows a cell voltage of 0.61 V close to steady-state and demonstrates a system with minimal loss of enzymatic activity.

Fig. 5 shows the polarization curves of the anode and cathode (obtained in potentiostatic regime) and the biofuel cell (galvanostatic regime). In the current operating range the cathode shows the typical behavior of an air breathing electrode with kinetic limitations at low currents, ohmic losses between 30 and 150 μA and a very sudden drop in potential at higher currents due to transport limitations imposed by the diffusion of air through the cathode

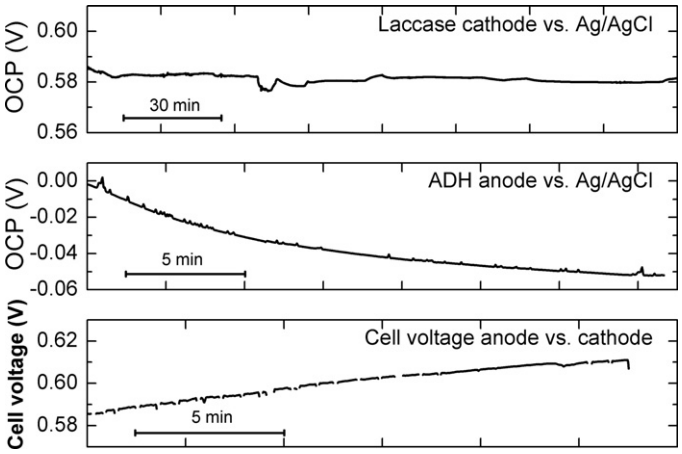

Fig. 4. Open circuit potentials of laccase-cathode and ADH-anode, and cell voltage of biofuel cell.

architecture. This biofuel cell sustained an OCV of 0.618 V, slightly higher than that of the MDH-laccase biofuel cell.

For both of the biofuel cell configurations studied the anode is the limiting electrode, and performance degradation mainly dictated by ohmic losses. The limitation is a consequence of various design aspects. Firstly, the supporting electrolyte contains a total salt concentration of 0.4 M, which compared to other electrochemical devices (e.g., batteries) is low. Enzymes however, could be inactivated at high salt concentrations, and as such, electrolyte optimization is a design parameter that could be addressed, but may inherently constrain the working limits of the system. Second, the 3D design and dimensions of the anode significantly separate the electrodes. This macroscopic separation (~1 cm) between the anode and the cathode and the flow of low conductive ions significantly contribute to the ohmic losses in the biofuel cell.

Fig. 6 shows power curves for the ADH-laccase biofuel cell in the same way as for the MDH-laccase. The maximum power density was determined to be ~25 μW cm^{-2} which is almost three times higher than that obtained for the MDH-laccase biofuel cell. In terms of volumetric density, the corresponding maximum power was ~21 μW cm^{-3}. This result is one order of magnitude higher than the one reported by Stoica et al. (2009) and at least double the

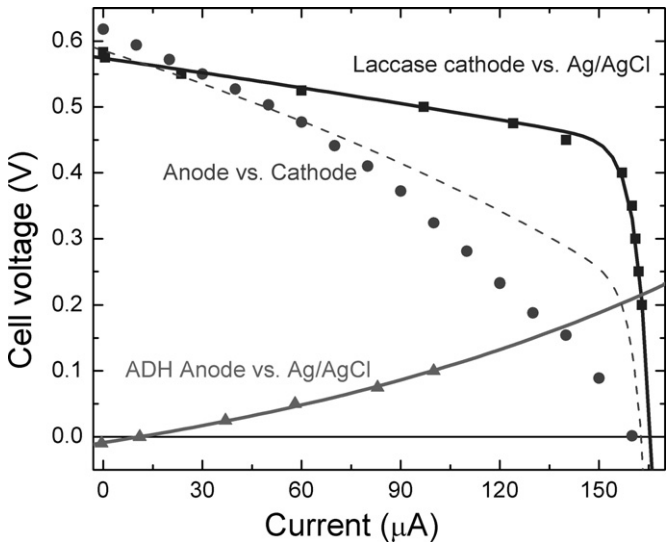

Fig. 5. Polarization curves of: (▲) ADH-anode, (■) laccase-cathode, and (●) biofuel cell. Dashed line represents the theoretical full cell polarization curve. Ethanol concentration: 475 mM. OCV = 0.618 V.

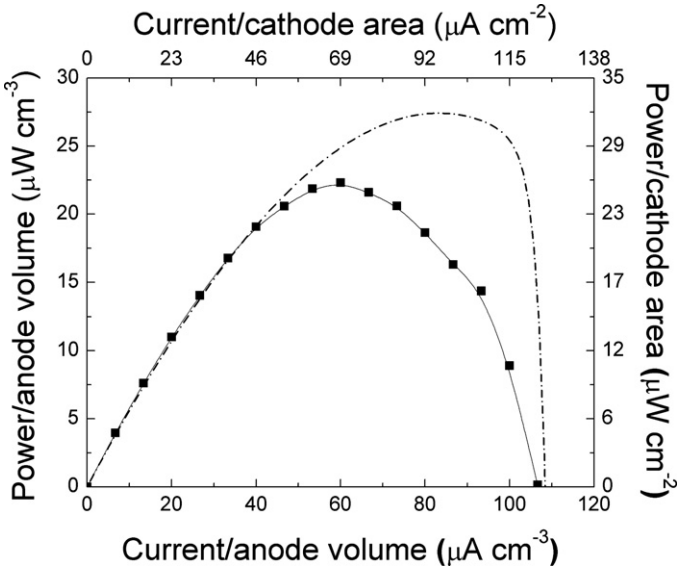

Fig. 6. Power curves of ADH-laccase biofuel cell in 475 mM ethanol normalized to anode volume and cathode area (dashed line: theoretical power curve, solid line: experimental power curve).

power obtained by Yan et al. (2006), for a single dehydrogenase biofuel cell in a mediated system.

Despite certain inherent limitations, the work described in this paper presents a functional yet not fully optimized biofuel cell with a single-enzyme anode and a single-enzyme cathode that serves as a platform for new biofuel cell designs and optimizations. The main advantage of the design platform that was studied is the ability to operate under flow through regime, where the fuel can be replenished and recycled for continuous operation.

Although the present system design allows for high residence time of the fuels due to the large dimensions of the anode, it has the disadvantage of macroscopic separation between the anode and cathode that contributes to a long path for ionic flow. Future directions of this research will include electrode architectures that offer an alternative design in which the separation between the cathode and anode could be minimized.

4. Conclusions

Two fully enzymatic biofuel cells based on single NAD^+-dependent dehydrogenase enzymes were constructed and evaluated in continuous flow-through operation. The MDH-laccase demonstrated some limitations in the anode performance that were reflected in a limiting current of ~65 μA, and maximum power densities approaching ~9 $\mu W\,cm^{-2}$ or ~8 $\mu W\,cm^{-3}$ (at 0.373 V). By comparison, upon substituting ADH for MDH; the ADH-laccase fuel cell showed higher performance output, achieving limiting currents ~160 μA and maximum power densities of ~26 $\mu W\,cm^{-2}$ or ~22 $\mu W\,cm^{-3}$ (at 0.372 V). The higher performance of the ADH-laccase is attributed to higher enzymatic activity of ADH that had previously been observed. This single-enzyme design serves as a model for future multiple-enzyme anodes that will have the capacity for multi-step oxidation of biofuels (increasing coulombic yield) and thus the potential to generate larger current and power densities.

Large ohmic losses characterized both anode configurations and resulted in polarization curves that exhibit resistive behavior. This ohmic effect was a consequence of the low conductivity of the supporting electrolytes as well as the macroscopic separation between the anode and the electrode. Improvements in design have been suggested including the utilization of electrode configurations that will allow juxtaposition of the anode and cathode, thereby reducing overall ohmic losses in the biofuel cell.

With this paper, we integrate the design efforts in both enzymatic anode and cathode that are product of various projects and collaborations. Furthermore, we have assembled these components into a device that allows continuous fuel cell operation in flow-through mode, as opposed to a quiescent mode in which the fuel is not replenished limiting the performance of the fuel cell. Designing of a biofuel cell aims minimizing the needs of energy use for any parasitic processes and a minimal balance of plant. The direction of our research is to move towards a passive transport in anode design that can be combined with air-breathing cathodes. The results of this study can also help identifying the challenges faced when a biofuel cell (as opposed to a "bio-battery") is being built – design of flow media for fuel supply, all immobilized components and integration with a minimal external energy-consuming components.

References

Barton, S.C., Gallaway, J., Atanassov, P., 2004. Chem. Rev. 104 (10), 4867–4886.
Barton, S.C., Kim, H.-H., Binyamin, G., Zhang, Y., Heller, A., 2001a. J. Phys. Chem. B 105 (47), 11917–11921.
Barton, S.C., Kim, H.H., Binyamin, G., Zhang, Y., Heller, A., 2001b. JACS 123 (24), 5802–5803.
Barton, S.C., Pickard, M., Vazquez-Duhalt, R., Heller, A., 2002. Biosens. Bioelectron. 17 (11–12), 1071–1074.
Chen, T., Barton, S.C., Binyamin, G., Gao, Z., Zhang, Y., Kim, H.H., Heller, A., 2001. JACS 123 (35), 8630–8631.
Cooney, M.J., Lau, C., Windmeisser, M., Liaw, B.Y., Klotzbach, T., Minteer, S.D., 2008. J. Mater. Chem. 18 (6), 667–674.
Cooney, M.J., Petermann, J., Lau, C., Minteer, S.D., 2009. Carbohydr. Polym. 75 (3), 428–435.
Davis, F., Higson, S.P.J., 2007. Biosens. Bioelectron. 22 (7), 1224–1235.
Ghindilis, A.L., Atanasov, P., Wilkins, E., 1997. Electroanalysis 9 (9), 661–674.
Gupta, G., Lau, C., Branch, B., Rajendran, V., Ivnitski, D., Atanassov, P., 2011a. Electrochim. Acta, doi:10.1016/j.electacta.2011.01.089.
Gupta, G., Lau, C., Rajendran, V., Colon, F., Branch, B., Ivnitski, D., Atanassov, P., 2011b. Electrochem. Commun. 13 (3), 247–249.
Heller, A., 2004. Phys. Chem. Chem. Phys. 6 (2), 209–216.
Ivnitski, D., Artyushkova, K., Atanassov, P., 2008. Bioelectrochemistry 74 (1), 101–110.
Ivnitski, D., Atanassov, P., 2007. Electroanalysis 19 (22), 2307–2313.
Ivnitski, D.M., Khripin, C., Luckarift, H.R., Johnson, G.R., Atanassov, P., 2010. Electrochim. Acta 55 (24), 7385–7393.
Katz, E., Shipway, A.N., Willner, I., 2003. In: Schmid, G. (Ed.), Nanoparticles—From Theory to Applications. Wiley-VCH, Weinheim, pp. 368–421.
Lau, C., Cooney, M.J., Atanassov, P., 2008. Langmuir 24 (13), 7004–7010.
Lau, C., Martin, G., Minteer, S.D., Cooney, M.J., 2010. Electroanalysis 22 (7–8), 793–798.
Mano, N., Soukharev, V., Heller, A., 2006. J. Phys. Chem. B 110 (23), 11180–11187.
Martin, G.L., Lau, C., Minteer, S.D., Cooney, M.J., 2010. Analyst 135 (5), 1131–1137.
Minteer, S.D., Liaw, B.Y., Cooney, M.J., 2007. Curr. Opin. Biotechnol. 18 (3), 228–234.
Morozova, O., Shumakovich, G., Gorbacheva, M., Shleev, S., Yaropolov, A., 2007. Biochemistry 72 (10), 1136–1150.
Palmore, G.T.R., Bertschy, H., Bergens, S.H., Whitesides, G.M., 1998. J. Electroanal. Chem. 443 (1), 155–161.
Piontek, K., Antorini, M., Choinowski, T., 2002. J. Biol. Chem. 277 (40), 37663–37669.
Reinhammar, B.R., 1972. Biochim. Biophys. Acta 275 (2), 245–259.
Rincón, R.A., Lau, C., Garcia, K.E., Atanassov, P., 2011. Electrochim. Acta 56 (5), 2503–2509.
Shleev, S., Tkac, J., Christenson, A., Ruzgas, T., Yaropolov, A.I., Whittaker, J.W., Gorton, L., 2005. Biosens. Bioelectron. 20 (12), 2517–2554.
Solomon, E.I., Baldwin, M.J., Lowery, M.D., 1992. Chem. Rev. 92 (4), 521–542.
Solomon, E.I., Sundaram, U.M., Machonkin, T.E., 1996. Chem. Rev. 96 (7), 2563–2605.
Stoica, L., Dimcheva, N., Ackermann, Y., Karnicka, K., Guschin, D.A., Kulesza, P.J., Rogalski, J., Haltrich, D., Ludwig, R., Gorton, L., Schuhmann, W., 2009. Fuel Cells 9 (1), 53–62.
Svoboda, V., Cooney, M., Liaw, B.Y., Minteer, S., Piles, E., Lehnert, D., Barton, S.C., Rincon, R., Atanassov, P., 2008. Electroanalysis 20 (10), 1099–1109.
Xu, F., Shin, W., Brown, S.H., Wahleithner, J.A., Sundaram, U.M., Solomon, E.I., 1996. Biochim. Biophys. Acta 1292 (2), 303–311.
Yan, Y.M., Zheng, W., Su, L., Mao, L.Q., 2006. Adv. Mater. 18 (19), 2639–2643.